Brief Communication

Co-seismic displacement on October 26 and 30, 2016 (M_w 5.9 and 6.5) - earthquakes in central Italy from the analysis of a local GNSS network

De Guidi Giorgio[1,2], Vecchio Alessia[1)], Brighenti Fabio[1], Caputo Riccardo[3,4,5], Carnemolla Francesco[1], Di Pietro Adriano[1], Lupo Marco[1], Maggini Massimiliano[3,5], Marchese Salvatore[1], Messina Danilo[1], Monaco Carmelo[1,2],Naso Salvatore[1]

1) Department of Biological, Geological and Environmental Sciences, University of Catania, Italy
2) CRUST, UR-UniCT, Catania, Italy
3) Department of Physics and Earth Sciences, University of Ferrara, Italy
4) Research and Teaching Center for Earthquake Geology, Tyrnavos, Greece
5) CRUST, UR-UniFE, Ferrara, Italy

Corresponding author: G. De Guidi (deguidi@unict.it)

1 - Abstract

On August 24th 2016 a strong earthquake (M_w = 6.0) affected Central Italy ~~starting~~ and an intense seismic sequence. Field observations, DInSAR analyses, preliminary focal mechanisms as well as the distribution of aftershocks suggested the reactivation of the northern sector of the Laga Fault, whose southern sector was already ~~reactivated~~ rebooted during the 2009 L'Aquila sequence, and of the southern segment of the Monte Vettore Fault System (MVFS). Based on these preliminary information and following the stress-triggering concept (Stein et al., 1999; Steacy et al., 2005), we tentatively identified a potential fault zone most vulnerable to future seismic events just north of the ~~first~~ earlier epicentral area. Accordingly, we planned a local geodetic network consisting of five new GNSS (Global Navigation Satellite System) stations located at few km of distance on both sides of the MVFS. This was devoted to picture out, at least partially but in some detail, the possible northward propagation of the crustal network ruptures. The building of the stations and a first set of measurements were carried out during a first campaign (September 30th-October 2nd, 2016). On October 26th 2016, immediately north of the epicentral area of the August 24th event, a ~~moderate~~ another earthquake (M_w = 5.9) indeed occurred, followed four days later (October 30th) by the mainshock (M_w = 6.5) of the whole 2016 Summer-Autumn seismic sequence. Our local geodetic network was fully affected by the new events and therefore we performed a second campaign soon after (November 11th-13th, 2016). In this brief note, we provide the results of our geodetic measurements that registered the co-seismic and immediately post-seismic deformation of the two major October shocks documenting in some detail the surface deformation close to the fault trace. We also compare our results with the available surface deformation field of the broader area, obtained on the basis of the DInSAR technique, and show~~ing~~ an overall good fit.

2 - Geological framework

The central Apennines are characterized by northeast-verging thrust-propagation folds, involving Mesozoic-Tertiary sedimentary successions. During the 2016 sequence, coseismic deformation was recorded at the rear of the Sibillini Thrust that separates the homonymous mountain chain from the Marche-Abruzzi foothills (Fig. 1). According to many studies in the area ~~affected by the recent earthquakes~~, the main thrust-related

anticlines and associated reverse faults have been dissected and/or inverted by NNW-SSE trending Quaternary normal and oblique-slip faults (Figs. 1 and 2), in particular by the Norcia Fault System (NFS) (Calamita and Pizzi, 1992; Calamita et al., 1982; 1995; 1999; 2000; Blumetti et al., 1990; Blumetti, 1995; Brozzetti and Lavecchia, 1994; Cello et al., 1998; Galadini and Galli, 2000; Pizzi and Scisciani, 2000; Pizzi et al., 2002; Boncio et al., 2004 Galadini, 2006; Gori et al., 2007) and the Mt. Vettore Fault System (MVFS) (Calamita and Pizzi, 1991; Coltorti and Farabollini, 1995; Cello et al., 1997; Pizzi et al., 2002; Galadini and Galli, 2003; Pizzi and Galadini, 2009) (Figs. 1 and 2). Conversely, Pierantoni et al. (2013) suggest that the major Mt. Sibillini Thrust has not been ~~not~~ yet dissected by quaternary normal faulting, though some fresh morphological scarps with free faces in the carbonate bedrock and/or affecting recent slope deposits have been observed and attributed to the local seismic activity.

Within a distance of few tens of kilometers, large evidence ~~of this Quaternary seismotectonic behaviour~~ ground deformation has been provided by several recent earthquakes, like the 1979 Norcia event (M_w 5.9, reactivating the Norcia Fault; e.g. Deschamps et al., 2000), the 1984 Gubbio (M_w 5.6, Gubbio Fault; e.g. Boncio et al., 2004), the 1997 Colfiorito ones (M_w 5.7, 6.0 and 5.6, Calfiorito-Cesi-Costa fault system; e.g. Cello et al., 1997), the 2009 L'Aquila mainshock and the Campotosto aftershock (M_w 6.3 and 5.4, Upper Aterno Valley-Paganica fault sytstem and Gorzano Fault; Blumetti et al. 2013) and basically the same occurred with the 2016 seismic sequence.

Surface evidence of the August 24th (e.g., EMERGEO WG, 2016; Livio et al., 2016; Aringoli et al., 2016) was mainly ~~occurred~~ observed in the area of the Laga basin (Gorzano Fault), which corresponds to the footwall block of Sibillini Thrust, while debated ground ruptures (e.g. Valensise et al., 2016) also occurred in the southern sector of the MVFS, which belongs to the hanging-wall block of the orogenic structure. In contrast, as a consequence of the mainshock of October 30th, the entire western flank of the Monte Vettore was affected by impressive geological effects and clear coseismic ruptures mapped for a minimum length of 15 km, between the Castelluccio di Norcia and Ussita (EMERGEO WG, 2016) (Fig. 2). The surface ruptures occured along distinct fault splays of the fracture system. For example, along the western slope of Monte Vettore three main west dipping splays were activated together with two antithetic branches (Figs. 1 and 2). The observed vertical offset reached 2 m along the main west dipping fault segment, where the slickensides show a prevalent dip-slip component of motion. Vertical displacements of a few centimetres were also recorded along an antithetic surface rupture bordering to the west the Castelluccio plain, about 6-7 km far from the main ground rupture, possibly connected to a secondary fault (Figs. 1B and 2).

It is worth to note that the August-October earthquakes occurred in a sector of the Central Apennines characterized by high geodetic strain-rates (e.g., Devoti et al., 2011; D'Agostino 2014), where several continuous GNSS stations are operating.

Implementation and Analysis of UNICT discrete GPS stations

Following the August~~,~~ 24th, M_W 6.0 earthquake, the GEOmatic Working Group of the Catania University (UNICT) in collaboration with the SpinOff EcoStat s.r.l. and researches of the Ferrara University, started a detailed monitoring of ground deformation in the epicentral area using the Global Navigation Satellite System (GNSS) technique. The GNSS measurement has been made in static mode, setting the time at 6 hours and post-processing position, in order to reduce tropospheric error and using IGS precise products for orbits. The IGS station coordinates were kept fixed in order to align the ~~fianl~~ final velocity field with the WGS84 reference frame. The measurement mode, adopted for receiver-satellite range determination, is performed with a double frequency receiver, allowing phase and code measurements on the signal carrier (L1, L2, C1, P1, P2, S1, S2). The coordinates estimation is based on the principle of minimum squares.

For this aim, five GNSS stations have been installed on new benchmarks purposely built by the working group and here referred to as UNICT network (Fig. 3). These new stations have been realized taking into account the following criteria:

I. the distribution of the existing permanent and discrete measurement benchmarks belonging to different networks that were active before the event of 24 August (IGM; RING; CAGEONET; DPC; ISPRA) (Fig. 2B).
II. the seismotectonic setting of the area in relation to the macroseismic data and to the reactivated structures (Figs. 1 and 2);
III. surface and deep geometry of the major faults related to tectonic setting (Fig. 1B).
IV. the lack of possible gravitational instabilities in both static and dynamic conditions in sites where the new benchmarks are built.

Based on the above criteria, the working group installed the benchmarks at the bottom of both western and eastern slopes of Mt. Vettore, within an area about 8 km-long and 5 km-wide in the N-S and E-W directions, respectively. The distribution of the benchmarks was planned for ~~depicting~~ reconstructing the principal deformation zone developed as a consequence of the August 24th~~,~~ event (Fig. 2 ~~and 3~~) and particularly with points:

I. much closer to the epicentral area than the already existing ones belonging to other networks (Fig. 2B);
II. characterized by equivalent distances from the reactivated Mt. Vettore Fault segments (Fig. 2);
III. within a distance of 30 km from the closest permanent network points that have been not affected by deformation, therefore allowing a rigorous elaboration during the post processing phases ~~(Fig. 3).~~

The ~~realization~~ building of G~~P~~NSS monument on the UNICT benchmarks consists of the following steps (Fig. 3):

I. selection of a suitable ~~point~~ site, corresponding to a massive rocky outcrop or a man-made monument with foundation; these sites must be also free of structures or other natural elements in the surroundings that may constitute a perturbation during recording;
II. testing of GPS signal reception by short-term exams, and control of parameters set ~~by~~ through the quality check carried out by software TEQC (http://www.unavco.org/software/data-processing/teqc/teqc.html);
III. implementation of the hole for housing the bushing and check of its verticality; the hole has a diameter of 35 mm and a depth of 100 mm, it is realized through small-sized battery-powered equipment (Makita DHR243 hammer drill) ~~(Fig. 3)~~;
IV. fixing and anchoring of the knurled steel bushing (length 67 mm and diameter 20 mm), with bi-component resins or quick-setting cements (Fig. 3);
V. following the cementation to the artefact or to rocky outcrop, a male-male threaded bar can be screwed in until end of stroke; the height could be variable and this fact ~~will be~~ is considered in the data processing. We have used a threaded bar 670 mm-high. ~~(Fig. 3).~~

The GPS monument is thus completed with a GNSS receiver TOPCON, mounting a HiPer V antenna, characterized by 226 channels and position accuracy with band L1+L2 in Static mode of 3 mm + 0.1 ppm (horizontal) and 3.5 mm + 0.4 ppm (vertical). All registrations last six hours in static mode.
Following the August 24th event, at the end of September 2016 the working group ~~have started~~ curried out the first survey campaign with the installation of five UNICT benchmarks: two stations were located east of

the Mt. Vettore fault (VTE1,VTE2), the other three (VTW3,VTW4, VTW5) west of the fault (Figs. 4 and 5). During November 2016 (*i.e.* after the October 30th event), a second field campaign was carried out following the same procedure and using the same instrumentation. The second set of measurements allowed ~~recording~~ us to record the co-seismic displacement caused by both the M_w 5.9 and M_w 6.5 events of October 26th and 30th, respectively (doy (day of year) 2016/274 and doy 2016/318).

The data from survey-mode GNSS stations have been downloaded and processed using TOPCON Magnet analysis software evaluating co-seismic solutions and comparing with AUSPOS web-based online services for GPS data processing (Ocalan et al., 2013), whose engine is based on Bernese 5.2 software. In the software TOPCON, the baseline is automatically created for any pair of static occupations, where we set up six hours for Minimum Duration and the baselines max length of 50 km, cut-off angle of 15°, troposphere model Goad-Goodman and, finally, meteo model NRLMSISE (neutral temperature and densities in Earth's atmosphere).

For the analyses we referred to the measurement of a stable reference frame of five GNSS stations belonging to the RING (Rete Integrata Nazionale GPS) network, with a maximum baseline length of 50 km, using stations CESI, GNAL, GUMA, MTER and MTTO (Figs. 4 and 5). Data processing has been carried out with adjustment by Least Squares and a TAU Criterion.

ID	Station	Longitudine	Latitudine	$disp_{N-S}$	$disp_{E-W}$	$disp_{UP}$	unc_{N-S}	unc_{E-W}	unc_{UP}
VTE1	FOCE_SENTIERO	13° 15' 57,45166''	42° 51' 57,04340''	141	312	29	15.5	16.5	44.0
VTE2	PRETARE	13° 16' 33,20959''	42° 47' 56,56780''	60	282	67	19.0	16.5	46.0
VTW3	QUARTUCCIOLO	13° 14' 46,41153''	42° 47' 56,57032''	198	26	-349	15.5	14.5	36.0
VTW4	COLLE_CURINA	13° 13' 55,01245''	42° 48' 59,62491''	102	288	-769	15.5	15.0	36.0
VTW5	CASTELLUCCIO_VALLE	13° 12' 56,20423''	42° 49' 54,89014''	353	418	-707	15.0	13.5	37.5

Tab 1 - Three components co-seismic displacements and relative uncertainties estimated for the GNSS stations of the UNICT network. Coordinates are WGS84 east and north, respectively. All displacement and uncertainty values are in millimeters. For all stations, the cut-off angle is 15°, the troposphere model is the Goad-Goodmar and the meteo model used is NRLMSISE. The table can be download as ASCII file on the INGVRING web page (http://ring.gm.ingv.it).

Concluding remarks

Using the GNSS technique, we investigated the ground deformation ~~that~~ occurred in the surroundings of the Mt. Vettore Fault System during the 2016 central Italy seismic sequence. This foresight action allowed us to record the co-seismic and part of the post-seismic deformation of the second and third (strongest) events (Mw 5.9 and M_W 6.5) on October 26th and October 30th, 2016, respectively. Taking into account the geometry of the fault system in the broader epicentral area and following the stress-triggering concept (Stein et al., 1999; Steacy et al., 2005), we have identified a potential fault zone most vulnerable to future seismic events just north of the fault segment reactivated during the August 24th earthquake (Figs. 2B and 5). With this in mind, in order to measure the post seismic deformation and to possibly record the potential migration of the co-seismic process, we selected some sites and built five new GNSS benchmarks, distributed east and west of the northern-central segment of the Mt. Vettore Fault System. For site selection we also considered the presence and distribution of other benchmarks located before the second seismic event by other research groups (IGM; RING; CAGEONET; DPC; ISPRA). The epicentral location of the October events ~~eventually~~ confirmed our guess and ~~we~~ then we performed soon after a second campaign of measurements for quantifying the relative motion of the stations.

The measured deformation (with 95% confidence errors) is characterised by both horizontal and vertical movements. In particular, the east benchmark VTE1 ~~documents~~ recorded 312 mm of eastward horizontal displacement and 29 mm of upward motion, while the VTE2 recorded 282 mm of eastward horizontal

displacement and 67 mm of upward component of motion. On the contrary, all three western benchmarks recorded westward horizontal displacements (419, 288 and 26 mm) and subsidence (707, 288 and 769 mm) for stations VTW5, VTW4 and VTW3, respectively. In conclusion, we documented ca. 730 mm of ENE-WSW lengthening on a distance of 7 km in correspondence of the northern sector of the Mt. Vettore Fault Segment, while the off-fault vertical displacement between footwall and hanging-wall blocks was 736 mm.

We also compared our results with the displacement distribution obtained by other research group with DInSAR techniques, recorded between October 26th 2016 (pre-event images) and November 1st 2016 (post-event images), and other GNSS stations, active before the second seismic event. In Fig. 5 we may observe the overall consistency of the different approaches and datasets.

Acknowledgments This paper was carried out with the financial support of the University of Catania (FIR 2014 Project Code 2C7D79, Scientific Supervisor: G. De Guidi) and University Spin Off of Catania EcoStat s.r.l.

References

Anzidei M., Baldi P. and Serpelloni E. (2008). The coseismic ground deformations of the 1997 Umbria-Marche earthquakes: A lesson for the development of new GPS networks, Ann. Geophys., 51(2–3), 27– 43.

Anzidei M. and Pondrelli S. (Eds) (2016). The Amatrice seismic sequence: preliminary data and results, Annals of Geophysics, 59, Fast Track 5, 2016

Aringoli D., Farabollini P., Giacopetti M., Materazzi M., Paggi S., Pambianchi G., Pierantoni P.P., Pistolesi E., Pitts A. and Tondi E. (2016). The August 24th 2016 Accumoli earthquake: surface faulting and Deep-Seated Gravitational Slope Deformation (DSGSD) in the Monte Vettore area. Ann. Geophysics, 59, fast track 5, 2016; doi: 10.4401/ag-7199.

Blumetti A.M. (1995). Neotectonic investigations and evidence of paleoseismicity in the epicentral area of the January-February 1703, Central Italy, earthquakes. In: Serva, L. & Slemmons, D. B., (eds.): Perspectives in paleoseismology. Association of Engineering Geologists, spec. publ. 6, 83-100.

Blumetti A.M., Dramis F., Gentili B. and Pambianchi G. (1990). La struttura di M. Alvagnano-Castel Santa Maria nell'area nursina: aspetti geomorfologici e sismicità storica. Rend. Soc. Geol. It., 13, 71-76.

Blumetti A.M., Guerrieri L. and Vittori E. (2013). The primary role of the Paganica-San Demetrio fault system in the seismic landscape of the Middle Aterno Valley basin (Central Apennines). Quaternary International, 288, 183-194, doi: 10.1016/j.quaint.2012.04.040.

Boncio P., Lavecchia G., and Pace B (2004). Defining a model of 3D seismogenic sources for Seismic Hazard Assessment applications: The case of central Apennines (Italy). Journal of Seismology 8: 407–425.

Brozzetti F. andLavecchia G. (1994). Seismicity and related extensional stress field; the case of the Norcia seismic zone (central Italy). Annales Tectonicae 8, 36–57

Calamita F. and Pizzi A., 1992. Tettonica quaternaria nella dorsale appenninica umbro-marchigiana e bacini intrappenninici associati. Studi Geologici Camerti, spec. vol. 1992/1, 17-25.

Calamita F., Coltorti M., Deiana G., Dramis F. and Pambianchi G. (1982). Neotectonic evolution and geomorphology of the Cascia and Norcia depression (Umbria-Marche Apennine). Geografia Fisica e Dinamica Quaternaria, 5, 263-276.

Calamita F., Pizzi A., Romano A., Roscioni M., Scisciani V. and Vecchioni G. (1995). La tettonica quaternaria nella dorsale appenninica umbro-marchigiana: una deformazione progressiva non coassiale. Studi Geol. Camerti, vol. spec.1995/1, 203-223.

213 Calamita F., Coltorti M., Pieruccini P. and Pizzi A. (1999). Evoluzione strutturale e morfogenesi plio-
214 quaternaria dell'appennino umbro-marchigiano tra il preappenino umbro e la costa adriatica. Bollettino
215 della Società Geologica Italiana, 118, 125-139.
216 Calamita F., Coltorti M., Piccinini D., Pierantoni P.P., Pizzi A., Ripepe M., Scisciani V. and Turco E. (2000).
217 Quaternary faults and seismicity in the Umbro-Marchean Apennines (central Italy). Journal of
218 Geodynamics 29, 245–264.
219 Cello G., Mazzoli S., Tondi E. and Turco E. (1997). Active tectonics in the Central Apennines and possible
220 implications for seismic hazard analysis in peninsular Italy. Tectonophysics, 272, 43-68.
221 Cello G., Deiana G., Mangano P., Mazzoli S., Tondi E., Ferreli L., Maschio L., Michetti A.M., Serva L. and Vittori
222 E. (1998). Evidence for surface faulting during the September 26, 1997, Colfiorito (Central Italy)
223 earthquakes. Journal of Earthquake Engineering, 2, 1-22.
224 Coltorti M. and Farabollini P. (1995). Quaternary evolution of the Castelluccio di Norcia Basin. Il Quaternario,
225 8, 149-166.
226 Deschamps A., Courboulex F., Gaffet S., Lomax A., Virieux J., Amato A., Azzara A., Castello B., Chiarabba C.,
227 Cimini G.B., Cocco M., Di Bona M., Margheriti L., Mele F., Selvaggi G., Chiaraluce L., Piccinini D. and
228 Ripepe M. (2000). Spatio-temporal distribution of seismic activity during the Umbria-Marche crisis, 1997.
229 Journal of Seismology 4: 377–386.
230 Devoti R., Esposito A., Pietrantonio G., Pisani A.R. and Riguzzi F. (2011). Evidence of large scale deformation
231 patterns from GPS data in the Italian subduction boundary. Earth and Planetary Science Letters, 311,
232 230–241, doi:10.1016/j.epsl.2011.09.034.
233 EMERGEO W.G. (2016). Coseismic effects of the 2016 Amatrice seismic sequence: first geological results.
234 Ann. Geophysics, 59, fast track 5, 2016; doi: 10.4401/ag-7195
235 Galadini F. and Galli P. (2000). Active tectonics in the Central Apennines (Italy) - Input data for seismic hazard
236 Assessment. Natural Hazards, 22, 225-270.
237 Galadini F. and Galli P. (2003). Paleoseismology of silent faults in the central Apennines (Italy): the Mt. Vettore
238 and Laga Mts. faults. Annali di Geofisica, 46, 815-836.
239 Galvani A., Anzidei M., Devoti R., Esposito A., Pietrantonio G., Pisani A., Riguzzi F. and Serpelloni E. (2012).
240 The interseismic velocity field of the central Apennines from a dense GPS network. Ann. Geophys. 55, 5,
241 2012; doi: 10.4401/ag-5634.
242 Gori S., Dramis F., Galadini F. and Messina P. (2007). The use of geomorphological markers in the footwall of
243 active faults for kinematic evaluations: examples from the central Apennines. Bollettino della Società
244 Geologica Italiana, 126, 365-374.
245 GdL-INGV (Gruppo di Lavoro INGV sul terremoto in centro Italia) (2016). Summary report on the October 30,
246 2016 earthquake in central Italy Mw 6.5, doi: 10.5281/zenodo.166238
247 Harris R.A. (1998). Introduction to special section: Stress triggers, stress shadows, and implications for seismic
248 hazard. J. Geophys. Res. 103, 347–358.
249 Kilb D., Gomberg J. and Bodin P. (2000). Triggering of earthquake aftershocks by dynamic stresses. Nature
250 408, 570–574.
251 Livio F., Michetti A.M., Vittori E., Gregory L., Wedmore L., Piccardi L., Tondi E., Roberts G. and Central Italy
252 Earthquake Working Grooup (2016): Surface faulting during the August 24, 2016, Central Italy
253 earthquake (Mw 6.0): preliminary results. Ann. Geophysics, 59, fast track 5, 2016; doi: 10.4401/ag-7197
254 Pierantoni P., Deiana G. and Galdenzi S. (2013). Stratigraphic and structural features of the Sibillini mountain
255 (Umbria-Marche- Appennines, Italy). Ital. J. Geosci. (Boll. Soc. Geol. It.) Vol.132 No.3, pp. 497-520.
256 Mantovani E., Viti M., Babbucci D., Cenni N., Tamburelli C., Vannucchi A., Falciani F., Fianchisti G., Baglione
257 M., D'Intinosante V. and Fabbroni P. (2011). Sismotettonica dell'Appennino Settentrionale. Implicazioni

per la pericolosità sismica della Toscana. Regione Toscana, Centro stampa Giunta Regione Toscana, Firenze, pagg. 88 (http://www.rete.toscana.it/sett/pta/sismica/index.shtml).

Pizzi A. and Galadini F. (2009). Pre-existing cross-structures and active fault segmentation in the northern-central Apennines (Italy), Tectonophysics, 476(1-2), 304–319, doi:10.1016/j.tecto.2009.03.018.

Pizzi A. and Scisciani V. (2000). Methods for determining the Pleistocene–Holocene component of displacement on active faults reactivating pre-Quaternary structures: examples from the central Apennines (Italy). Journal of Geodynamics 29, 445–457.

Pizzi A., Calamita F., Coltorti M. and Pieruccini P. (2002). Quaternary normal faults, intramontane basins and seismicity in the Umbria-Marche- Abruzzi Apennine ridge (Italy): contribution of neotectonic analysis to seismic hazard assessment. Boll. Soc. Geol. It., Spec. Publ., 1, 923–929.

Pizzi A., Calamita F., Coltorti M. and Pieruccini P. (2002). Quaternary normal faults, intramontane basins and seismicity in the Umbria-Marche- Abruzzi Apennine ridge (Italy): contribution of neotectonic analysis to seismic hazard assessment. Boll. Soc. Geol. It., Spec. Publ., 1, 923–929.

Pizzi A. and Galadini F. (2009) Pre-existing cross-structures and active fault segmentation in the northern-central Apennines (Italy). Tectonophysics. 476, 304-319.

Steacy S., Gomberg J. and Cocco M. (2005). Introduction to special section: Stress transfer, earthquake triggering, and time-dependent seismic hazard. J. Geophys. Res. 110, B05S01.

Stein R.S. (1999).The role of stress transfer in earthquake occurrence. Nature 402, 605–609.

Valensise G., Vannoli P., Basili R., Bonini L., Burrato P., Carafa M.C., Fracassi U., Kastelic V., Maesano F.E., Tiberti M. and Tarabusi G. (2016). Fossil landscapes and youthful seismogenic sources in the central Apennines: excerpts from the 24 August 2016, Amatrice earthquake and seismic hazard implications. Ann. Geophysics, 59, fast track 5, 2016; doi: 10.4401/ag-7215.

Website links

http://iside.rm.ingv.it

http://ring.gm.ingv.it

http://www.igmi.org/geodetica/

http://www.irea.cnr.it/index.php?option=com_k2&view=item&id=761:nuovi-risultati-sul-terremoto-del-30-ottobre-2016-ottenuti-dai-radar-dei-satelliti-sentinel-1

http://www.irea.cnr.it/index.php?option=com_k2&view=item&id=761:nuovi-risultati-sul-terremoto-del-30-ottobre-2016-ottenuti-dai-radar-dei-satelliti-sentinel-1

http://www.isprambiente.gov.it

http://www.unavco.org/software/data-processing/teqc/teqc.html

Rete Integrata Nazionale GPS - http://ring.gm.ingv.it/

http://terremoti.ingv.it/it/ultimi-eventi/1001-evento-sismico-tra-le-province-di-rieti-e-ascoli-p-m-6-0-24-agosto.html; Sequenza sismica di Amatrice, Norcia, Visso: approfondimenti e report scientifici

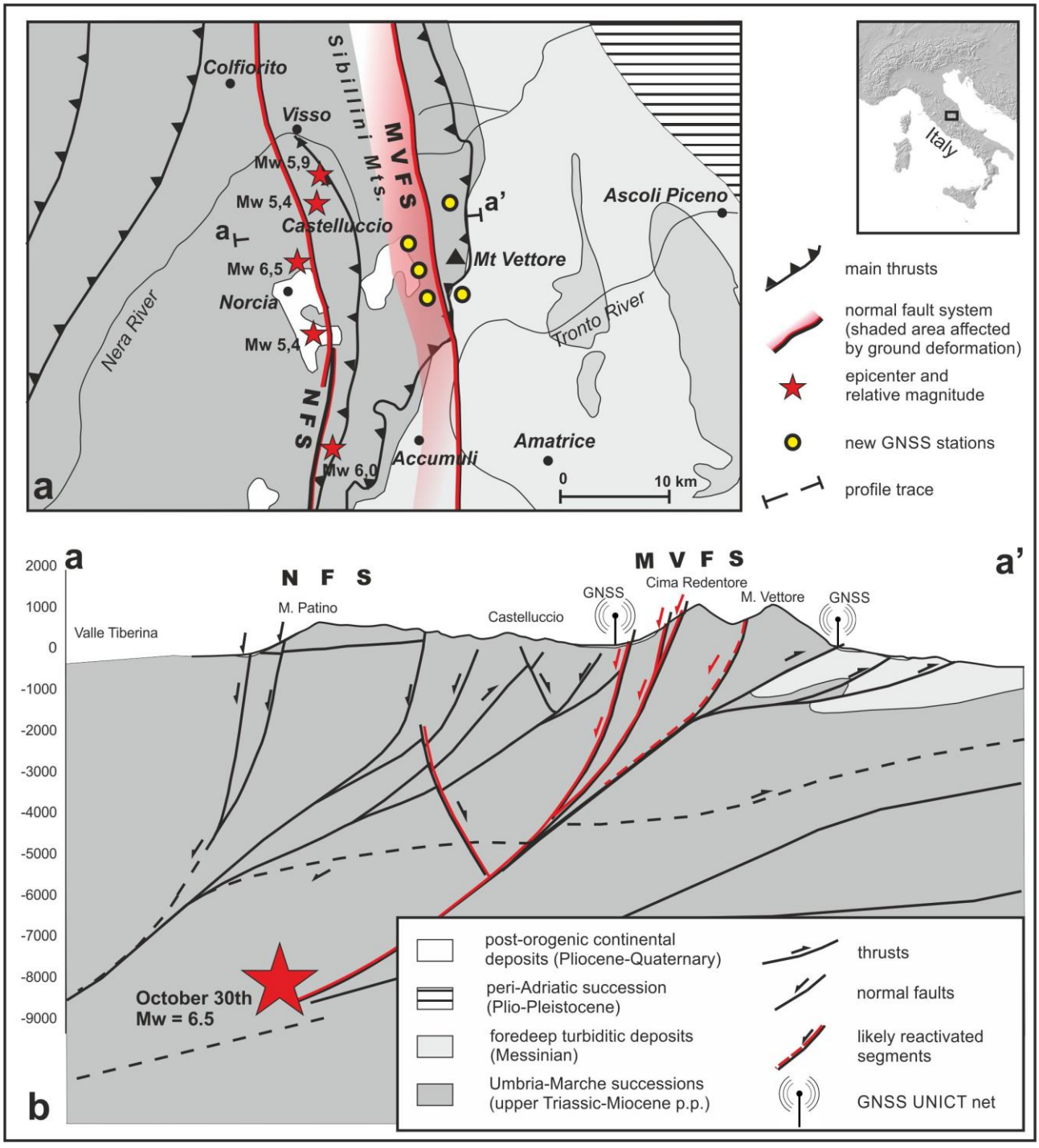

Fig. 1 Simplified seismotectonic map of central Apennines (A) and geological profile across the epicentral area (B). The location of the major event (October 30th) is from GdL INGV (2016), while the main geostructural features from Pierantoni et al. (2013) and Mantovani et al. (2011) modified).

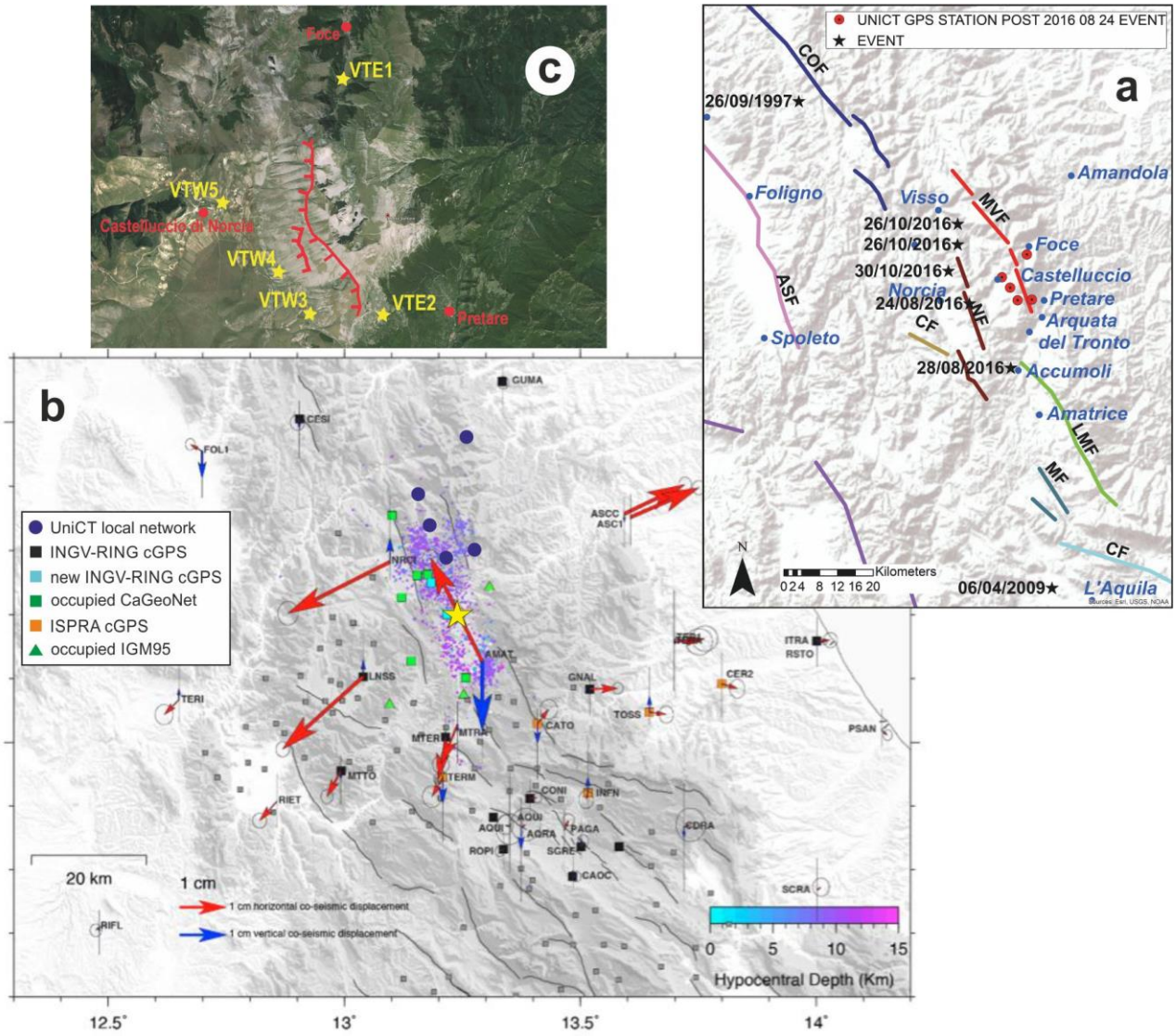

Fig. 2 – a) Digital Elevation Model with shaded relief of central Apennines showing the active fault system and the major events since 1997 (ASF: Assisi Fault; COF: Colfiorito Fault; CF: Cascia Fault; MVF: Mt. Vettore Fault; NF: Norcia Fault; LMF: Laga Mts. Fault; MF: faults of the Montereale basin). b) Horizontal (red arrows) and vertical (blue arrows) consensus co-seismic displacements (with 68% confidence errors), and the local UniCT GPS network. The aftershocks of the August 24th, Mw 6.0 main event (yellow star) are colored as a function of depth (from http://iside.rm.ingv.it); c). GoogleEarth map showing the new five GNSS stations (yellow stars) located in the near field of (and surrounding) the October 30th coseismic ground ruptures (red lines).

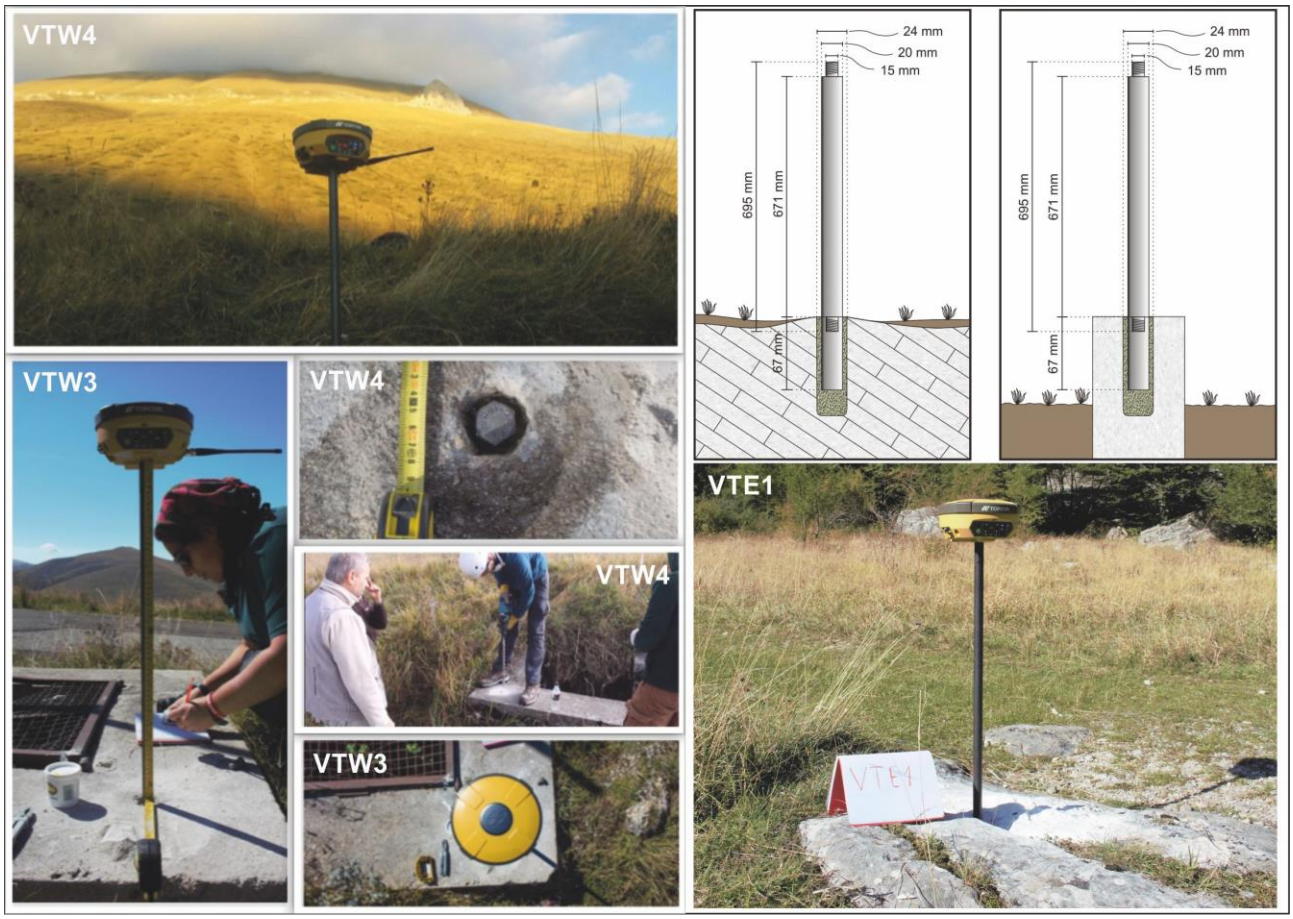

Fig. 3 Synoptic picture showing installation of the new GNSS stations, measurement and processing phases.

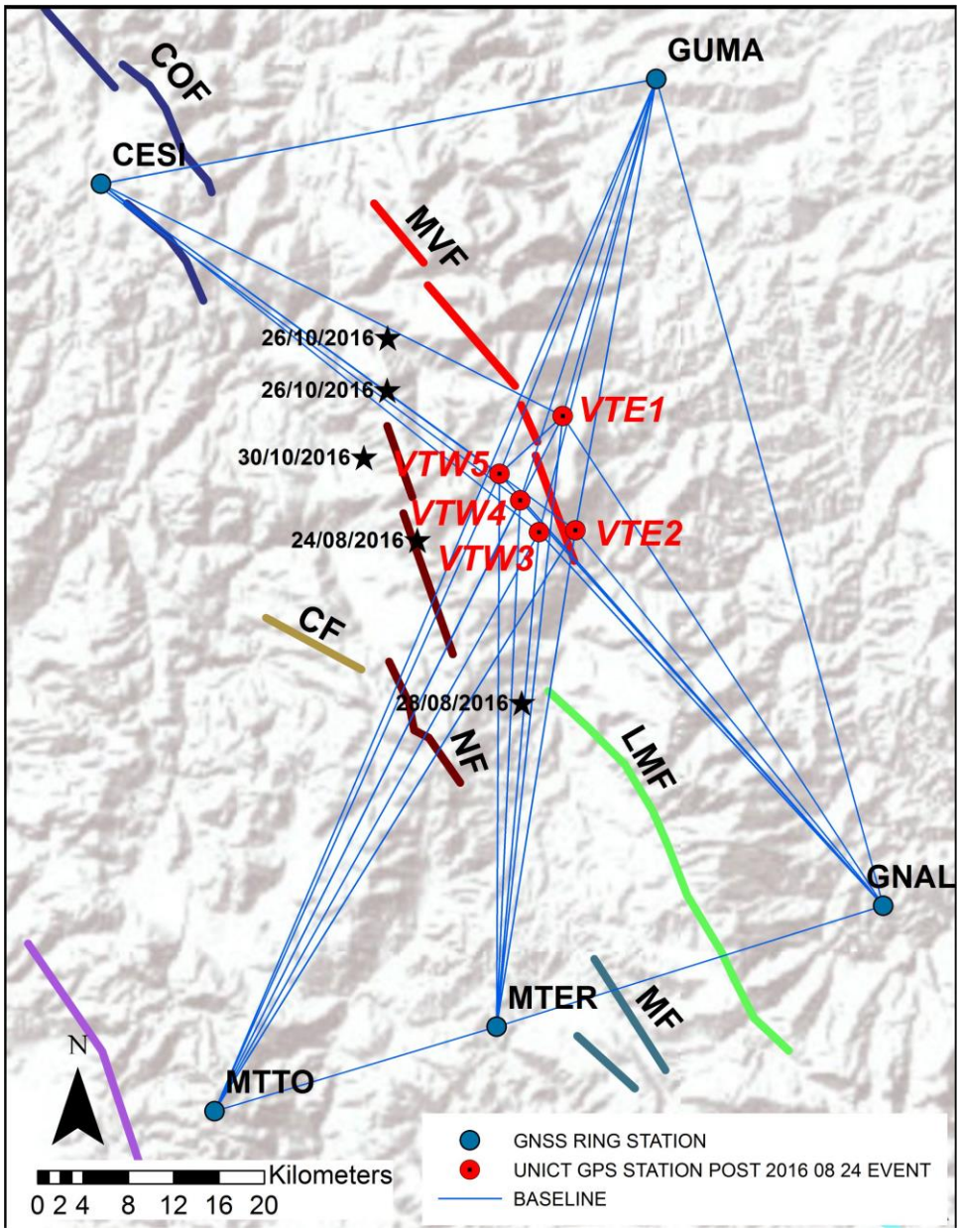

Fig. 4 Baselines obtained by combining the new GPS UNICT stations with selected GNSS ones from the RING Network.

---------->

Fig. 5 Color-coded maps showing the E-W (a) and vertical (b) displacement distribution obtained by the DInSAR technique (http://www.irea.cnr.it/index.php?option=com_k2&view=item&id=761:nuovi-risultati-sul-terremoto-del-30-ottobre-2016-ottenuti-dai-radar-dei-satelliti-sentinel-1) recorded On October 26th 2016 (pre-event images) and on November 1st 2016 (post-event images).The red and blu arrows represent the consensus pre-, co-, and post-seismic displacements (with 95% confidence errors) on the basis of the GNSS UNICT network. Epicenters of major shocks are from http://ring.gm.ingv.it.

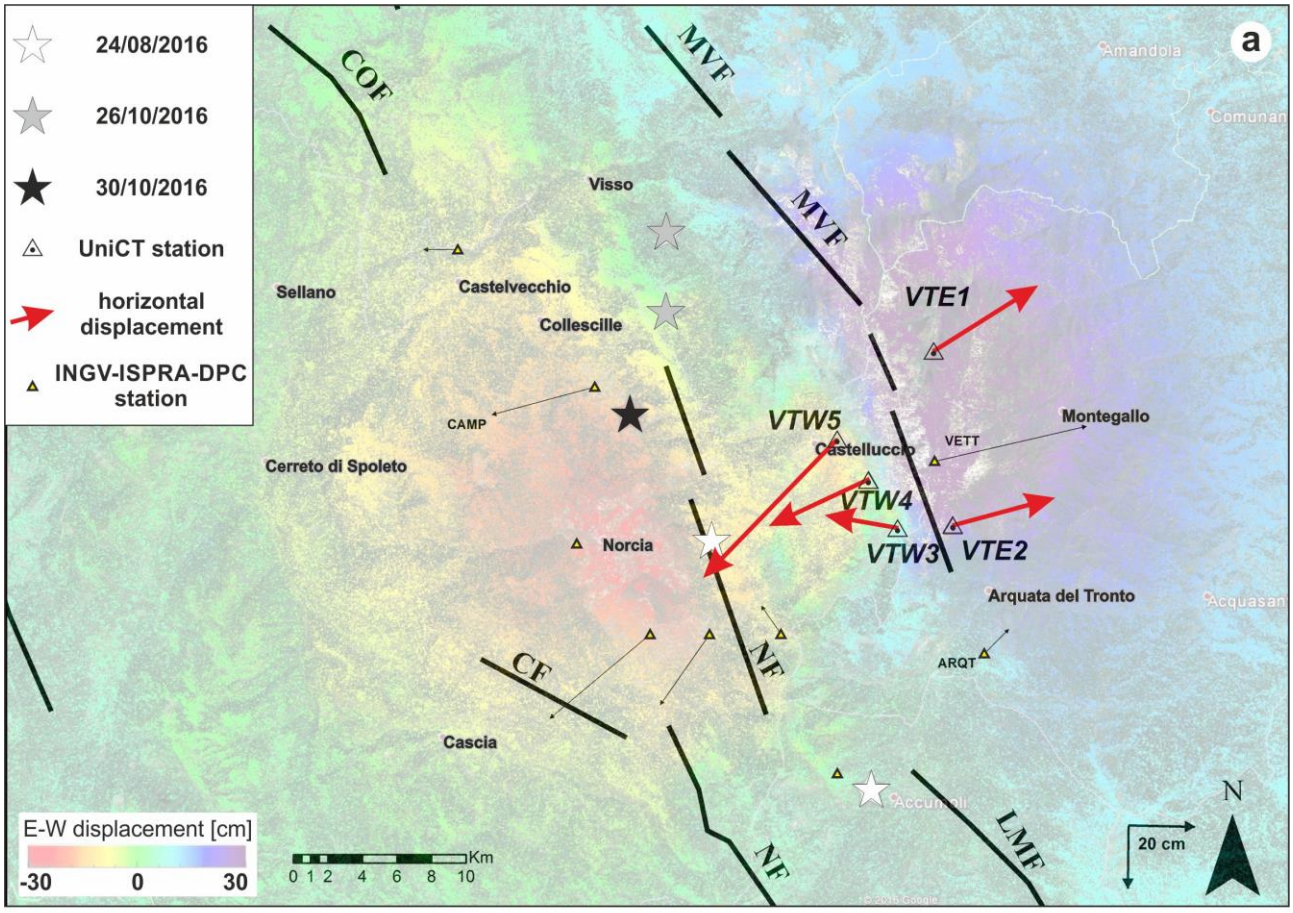
a
24/08/2016
26/10/2016
30/10/2016
UniCT station
horizontal displacement
INGV-ISPRA-DPC station
COF
MVF
MVF
Visso
Sellano
Castelvecchio
Collescille
CAMP
Cerreto di Spoleto
VTE1
VTW5
Castelluccio
VETT
Montegallo
VTW4
VTW3
VTE2
Norcia
Arquata del Tronto
ARQT
CF
NF
Cascia
NF
LMF
E-W displacement [cm]
-30 0 30
0 1 2 4 6 8 10 Km
20 cm
N

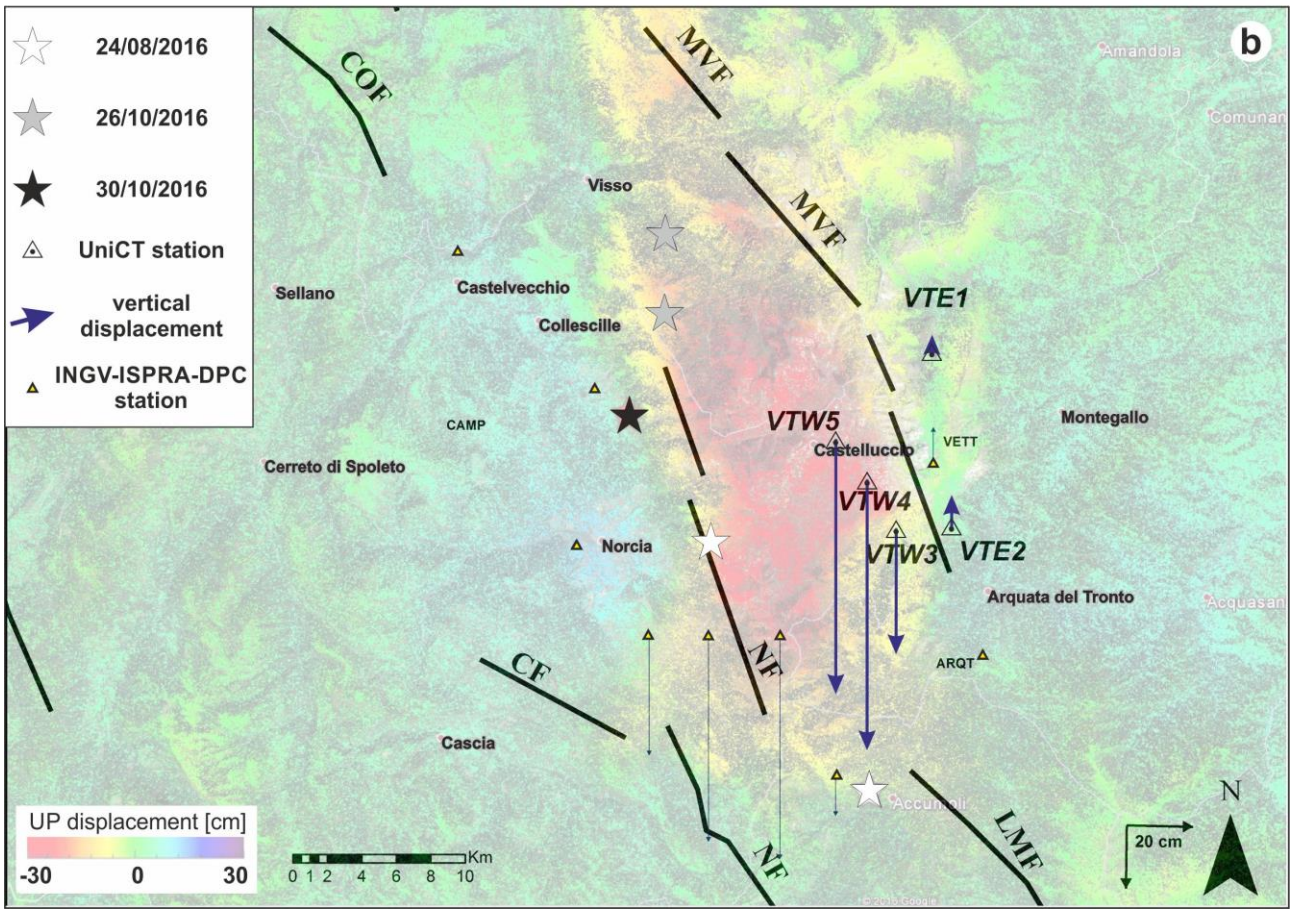
b
24/08/2016
26/10/2016
30/10/2016
UniCT station
vertical displacement
INGV-ISPRA-DPC station
COF
MVF
MVF
Visso
Sellano
Castelvecchio
Collescille
CAMP
Cerreto di Spoleto
VTE1
VTW5
Castelluccio
VETT
Montegallo
VTW4
VTW3
VTE2
Norcia
Arquata del Tronto
ARQT
CF
NF
Cascia
NF
LMF
UP displacement [cm]
-30 0 30
0 1 2 4 6 8 10 Km
20 cm
N